Part 5:
Relevance of winds on stellar/planetary evolution

https://doi.org/10.1017/S1743921322004446 Published online by Cambridge University Press

Winds of Stars and Exoplanets
Proceedings IAU Symposium No. 370, 2023
A. A. Vidotto, L. Fossati & J. S. Vink, eds.
doi:10.1017/S1743921322004446

Role of planetary winds in planet evolution and population

D. Modirrousta-Galian

Yale University Department of Earth and Planetary Sciences, 210 Whitney Ave., New Haven, CT 06511, USA

Abstract. The role of atmospheric evaporation in shaping exoplanet populations remains a major unsolved problem in the literature. Observational evidence, like the bimodal distribution of exoplanet radii, suggests a catastrophic past in which exoplanets with masses of approximately $1-10M_{\oplus}$ often lose their primordial envelopes and experience a drastic reduction in their radii. Our knowledge of the mechanisms behind atmospheric evaporation remains nebulous, with new models regularly introduced in the literature. Understanding the principles behind these models and knowing when to apply them is essential for constraining how planets evolve. This communication reviews the mechanisms behind atmospheric evaporation by exploring observations and theory, as well as introducing some of the principles in the forthcoming paper Modirrousta-Galian & Korenaga (in press).

Keywords. Mini Neptunes(1063) — Super Earths(1655) — Star-planet interactions(2177) — Exoplanet evolution(491) — Exoplanet atmospheres(487) — Planetary interior(1248)

1. Introduction

The first exoplanet was discovered in 1995 (Mayor & Queloz 1995) and, since then, the total number of known exoplanets has surpassed five thousand as of writing. The flourishing of the observational exoplanet sector has led to numerous surprising discoveries. One such finding is that atmospheric evaporation shapes the histories and evolutions of exoplanets in their totality. This discovery led to a surge in the popularity of atmospheric evaporation research and the generation of various mass loss models. In this communication, I focus on the two main sources of atmospheric evaporation: core powered mass loss (e.g., Ginzburg et al. 2018) and X-ray and ultraviolet irradiation (e.g., Micela et al. 2022). Other mass loss mechanisms, such as mechanical impact erosion (e.g., Cameron 1983; Ahrens 1993; Genda & Abe 2005; Schlichting et al. 2015) and coronal mass ejections (e.g., Cohen et al. 2011; Hazra et al. 2022), will not be discussed. This communication provides a short review of the data and theory of atmospheric evaporation for a nonspecialist audience. I will first discuss the available data and theory before the Second Light (K2) mission in 2014. I will then summarize the current state of research in the atmospheric evaporation literature. In the last section, I will explore possible future directions and conclude. Throughout this writing, the structure of planets will be categorized in two parts: (1) The central condensed section of the planet will be called the embryo (i.e., the silicate mantle with the central metallic core) and (2) the primordial atmosphere. A full theoretical framework is provided in the forthcoming paper Modirrousta-Galian & Korenaga (in press).

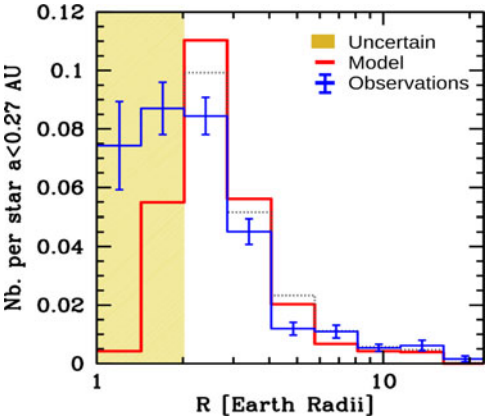

Figure 1. The radius distribution of exoplanets with periods less than 50 days (a<0.27 AU for a $1M_*$ star). The line without error bars shows their synthetic population, the line with error bars marks the data from Howard et al. (2010), Borucki et al. (2011), and Batalha et al. (2011), and the shaded region is uncertain. The age of the synthetic population is 5 Gyr. Figure adapted from Mordasini et al. (2012).

1.1. *The past*

Data on exoplanet population trends was limited before the launch of the Kepler mission in 2009 because most known exoplanets were hot Jupiters, so our understanding was based mostly on theoretical principles with origins in the Earth and planetary science field (e.g., Armitage 2014). Formation simulations indicate that the occurrence rate of planetary embryos inversely scales with their masses, that is, smaller mass embryos are more abundant than heavier ones (e.g., Ida & Lin 2004, 2005; Baraffe et al. 2006). In addition, gas accretion simulations suggest that exoplanets usually acquire atmospheres that are ∼1% of their total masses (e.g., Ikoma & Hori 2012; Lee et al. 2014), though there is a large variance (e.g., Ikoma et al. 2000). By combining the predicted embryo mass distribution with their expected atmospheric masses, it was thought that the radius distribution of exoplanet radii would follow a skewed Gaussian (e.g., Mordasini et al. 2012). Figure 1 shows the predicted radius distribution according to the simulations of Mordasini et al. (2012) plotted with the available data at the time (Howard et al. 2010; Borucki et al. 2011; Batalha et al. 2011).

The number of known exoplanets grew significantly after the activation of the Second Light (K2) mission in 2014 (e.g., Burke et al. 2014). It was found that, rather than being Gaussian, the radius distribution was bimodal with one peak at $1.3R_\oplus$, the other peak at $2.4R_\oplus$, and the minimum point at $1.75R_\oplus$ (Fulton et al. 2017). The statistical robustness of the distribution suggested that the peaks were the manifestations of two distinct exoplanet populations: one without primordial atmospheres called super-Earths and the other with primordial atmospheres called sub-Neptunes (see Figure 2). This was further evidenced by the paucity of planets with large radii and orbital periods less than three days (i.e., the sub-Jovian desert; Fulton et al. 2017), indicating a hidden mechanism that causes planets to experience a significant reduction in their radii through their lifetimes (e.g., Owen & Lai 2018).

Three mechanisms have been proposed to explain the bimodal distribution and sub-Jovian desert. The first is core powered mass loss, which suggests that a planet acquires a large amount of energy after its giant impact phase of formation that triggers extreme mass outflow (e.g., Ginzburg et al. 2018; Biersteker & Schlichting 2019). The second argument is that X-ray and ultraviolet (XUV) irradiation from stars ionizes and heats

https://doi.org/10.1017/S1743921322004446 Published online by Cambridge University Press

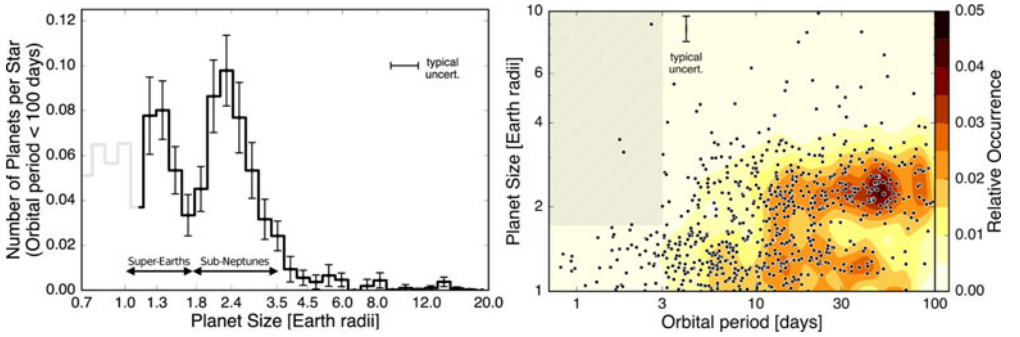

Figure 2. *Left:* The bimodal distribution of exoplanet radii. The data has been corrected for completeness. The lighter grey region for $R<1.14R_\oplus$ suffers from low completeness. The $1-1.75R_\oplus$ and $1.75-3.5R_\oplus$ regions are super-Earths and sub-Neptunes, respectively. *Right:* The sub-Jovian desert (the dark shaded area for periods less than three days and radii larger than $1.75R_\oplus$). Both figures have been adapted from Fulton et al. (2017).

the thermospheres of planetary atmospheres, causing their loss (e.g., Owen & Wu 2017; Modirrousta-Galian et al. 2020). The final argument proposes that the bimodal distribution is a natural outcome of planet formation in which the two peaks are comprised of rocky and ice-rich planets, respectively (e.g., Zeng et al. 2019; Venturini et al. 2020). The following section explores the core powered and XUV evaporation models. The formational argument for the bimodal distribution and sub-Jovian desert will not be further discussed because this communication focuses on the role of planetary winds and not cosmochemistry or planetary formation.

1.2. *The present*

There is an ongoing discussion on whether core powered mass loss or X-ray and ultraviolet irradiation are responsible for the bimodal distribution and sub-Jovian desert. Both models predict greater mass loss rates in the early stages of a planet's life because stars and planets are more energetic immediately after formation. The core powered and XUV-induced mass loss models will be qualitatively discussed below.

1.2.1. Core powered mass loss

The core powered mass loss model builds on concepts that originated in the Earth and planetary science field (e.g., Armitage 2014), where it has long been suggested that planets the size of Earth and larger experience a giant impact phase in which planetesimals collide and merge, leading to extreme surface temperatures. Simulations suggest that Earth could have had temperatures above 10,000 K (e.g., Karato 2014; Nakajima & Stevenson 2015; Lock et al. 2018) and, because super-Earths and sub-Neptunes have greater masses than Earth, they probably experienced more giant impacts and had higher surface temperatures. There is no simple analytic formula for estimating the mass loss rate of a planet experiencing core powered mass loss because the atmospheric dynamics will change depending on the internal state of the embryo. Only by creating a fully self-consistent planetary model can core powered mass loss be estimated.

Ginzburg et al. (2018) was the first to propose that a super-Earth or sub-Neptune could experience an extreme loss of primordial gases after a giant impact (see Figure 3). They suggest that the core powered mass loss mechanism can remove the light envelopes of small planets but not the heavy envelopes of larger ones, leading to the bimodal distribution of exoplanet radii. Their numerical framework assumes that the magma

https://doi.org/10.1017/S1743921322004446 Published online by Cambridge University Press

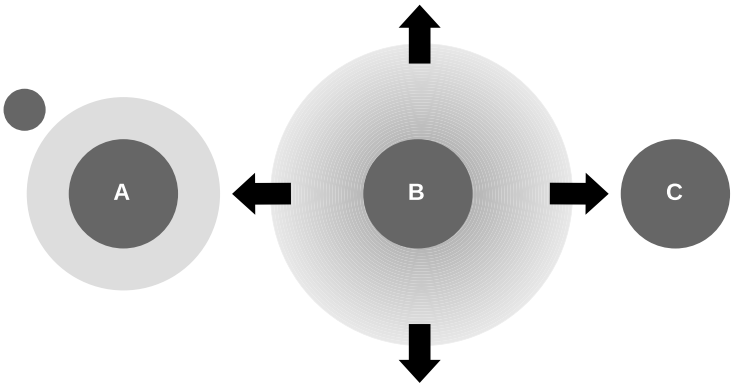

Figure 3. Schematic diagram showing the core powered mass loss mechanism. *A* shows a protoplanet with a primordial atmosphere immediately before a giant impact. *B* shows how the atmosphere expands because of the large amount of internal energy deposited from the giant impact. *C* shows a possible final outcome in which the entire atmosphere is lost.

ocean is isothermal, which is adequate as a first-order approximation, but a more realistic treatment would be needed if a detailed analysis is desired (e.g., Miyazaki & Korenaga 2019). Magma is composed of a mixture of minerals, so rather than crystallizing at a single temperature like water, it has a range of temperatures over which crystallization occurs (e.g., Solomatov 2015). Three points in this temperature range are of notable importance: (1) The liquidus is defined as the lowest temperature at a given pressure where magma is fully molten, (2) The solidus is the highest temperature at a given pressure where magma is fully crystallized, and (3) the rheological transition is the temperature at a given pressure where magma transitions from behaving rheologically like a liquid to a solid. A magma ocean can cool efficiently only when its surface temperature exceeds the rheological transition; convection will be sluggish and cooling inefficient at temperatures below it. By not including the effects of rheology in their magma ocean model, the internal energy available to drive atmospheric evaporation was overestimated.

Regarding observational data, the core powered mass loss model cannot explain the sub-Jovian desert because it defines mass loss only by the internal conditions of the embryo. In other words, this model is independent of the orbital period of the planet or the type of star it orbits. The inability of the core powered mass loss model to explain the sub-Jovian desert has been used as a justification for ignoring the internal heat flux as a source of mass loss. In the next section, the XUV-induced photoevaporation mechanism is examined in the absence of interior energy.

1.2.2. X-ray and ultraviolet mass loss

X-ray and ultraviolet induced photoevaporation (see Figure 4) has long been discussed in the Earth and planetary science literature (e.g., Watson et al. 1981; Hunten et al. 1987). Its application to exoplanets was popularized by Owen & Wu (2013, 2017), who suggested that the bimodal distribution can be explained by a population of exoplanets with masses of approximately $3M_{\oplus}$, where half have primordial atmospheres and the other half do not. The sub-Jovian desert is straightforward to explain with XUV-induced photoevaporation because closely orbiting planets are more highly irradiated than further orbiting ones, so they are more prone to total atmospheric loss. Owen & Wu (2013, 2017) used the energy limited approximation (Watson et al. 1981; Erkaev et al. 2007) for estimating mass loss, which does not incorporate thermal heating from the star's bolometric flux because it assumes that only XUV irradiation drives outflow. Indeed, fluid dynamical simulations

https://doi.org/10.1017/S1743921322004446 Published online by Cambridge University Press

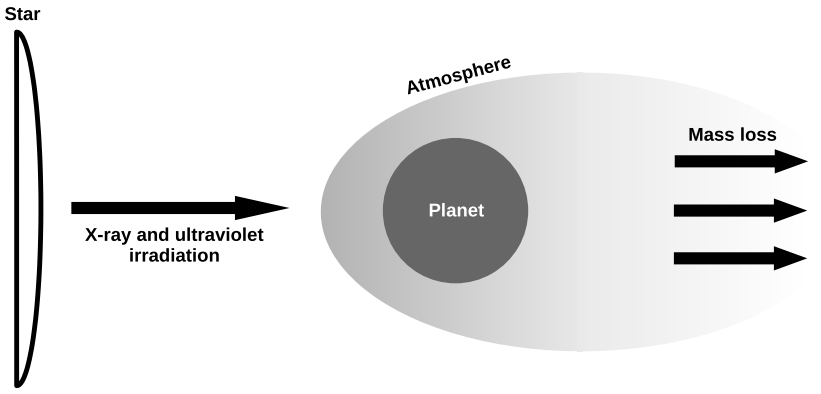

Figure 4. Schematic diagram showing the configuration of a planet experiencing atmospheric evaporation because of X-ray and ultraviolet irradiation.

show that the energy limited approximation underestimates mass loss rates by several orders of magnitude (e.g., García Muñoz 2007; Tian 2015; Caldiroli et al. 2021) and should not be used for highly irradiated super-Earths and sub-Neptunes.

Because the mass loss rates predicted by hydrodynamic models are substantially different from those of the energy limited approximation, it was not obvious if the bimodal distribution and sub-Jovian desert were still reproducible through XUV-induced photoevaporation alone. Modirrousta-Galian et al. (2020) tackled this problem by running a population simulation using the models of Kubyshkina et al. (2018a,b). Their findings suggested that the masses of exoplanets had to be larger than those predicted by Owen & Wu (2017) for the bimodal distribution to form. Their best fit mass distribution had few planets with masses less than three Earth masses, a uniform distribution between three and eight Earth masses, and a decrease in the occurrence rate of exoplanets with masses above eight Earth masses. The simulations of Modirrousta-Galian et al. (2020) implied that XUV irradiation alone could explain observations without requiring other mass loss mechanisms, such as the core powered mass loss model. However, the discovery of super-Earths and sub-Neptunes with densities lower than cold hydrogen gas (called super-puffs) provided renewed support for the core powered mass loss mechanism because such enlarged radii can be attained only with high internal luminosities. Figure 5 shows the mass and radius plots of DS Tuc A b and the planets in the Kepler-51 system (Libby-Roberts et al. 2020; Benatti et al. 2019, 2021). In other words, a combination of photoevaporation and core powered mass loss is required to explain the bimodal distribution, sub-Jovian desert, and super-puff presence.

1.3. *The future*

Core powered mass loss and XUV-induced photoevaporation are endmember cases for atmospheric evaporation. The first models mass loss arising from the internal luminosity of the planet, and the other models the mass loss from incoming stellar irradiation. Fluids behave very differently depending on whether they are heated from above or below, so the incoming and outgoing energy fluxes need to be considered concurrently when modeling mass loss. For example, fluids are prone to Rayleigh-Bénard convection when heated from below, whereas heating from above causes them to become stably stratified. The balance between the outgoing and incoming energy fluxes will influence the thermal structure of the entire planet. By considering the internal and incoming luminosity, it can be shown that mass loss is neither purely XUV driven nor purely core powered but a mixture of both.

https://doi.org/10.1017/S1743921322004446 Published online by Cambridge University Press

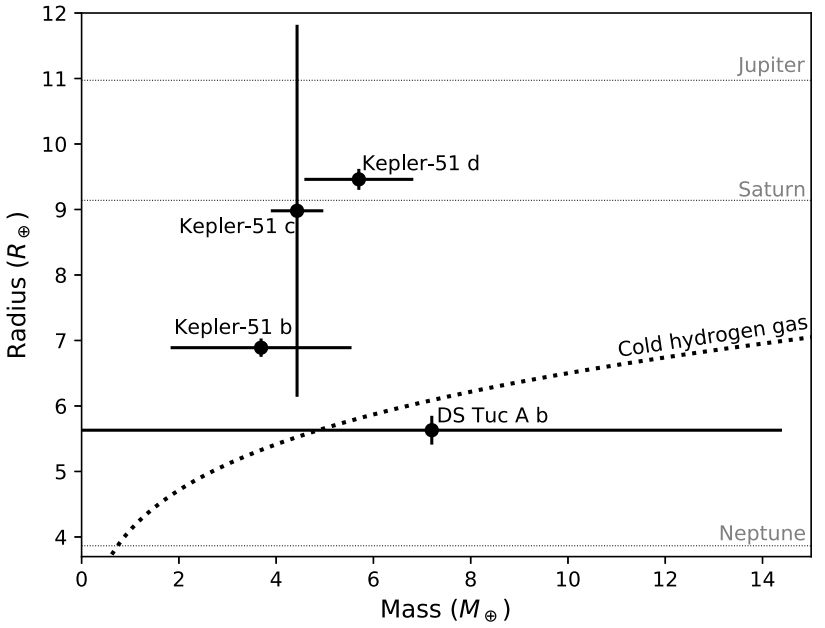

Figure 5. Mass and radius of Kepler-51 b, c, d (Libby-Roberts et al. 2020), and DS Tuc A b (Benatti et al. 2019, 2021). The cold hydrogen gas curve is from Zeng et al. (2019) who used the equation of state data of Becker et al. (2014).

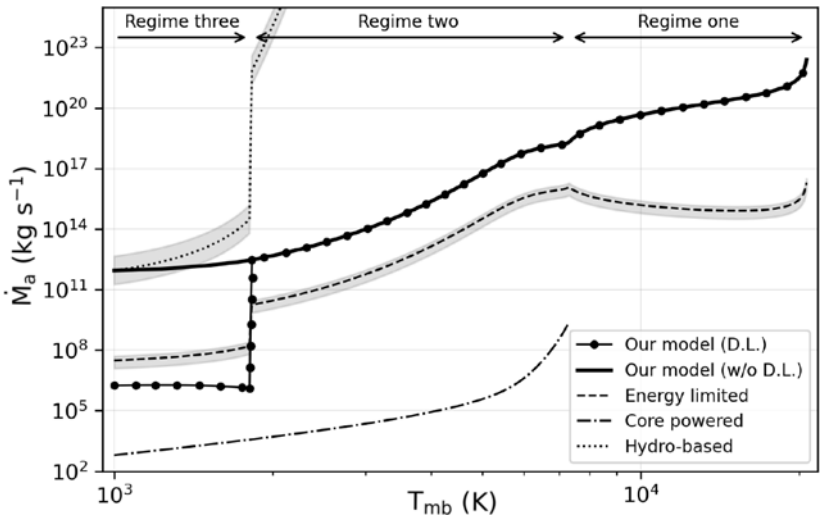

Figure 6. The predicted atmospheric evaporation rates as a function of the temperature of the boundary layer of the magma ocean ($T_{\rm mb}$) for an exoplanet that is three times the mass of Earth with a core-mass fraction of 26%, a primordial (hydrogen-rich) atmosphere that is 1% of the total planetary mass, an equilibrium temperature of 500 K, and experiencing an XUV radiant flux of 0.1 W m^{-2}. The black solid with circles, thick black solid, dashed, dash-dotted, and dotted lines are for our model with and without the diffusion limited mass loss included, the energy limited model (Watson et al. 1981), the core powered model (Biersteker & Schlichting 2019, 2021), and the hydro-based model (Kubyshkina et al. 2018a,b). The gray regions mark the typical uncertainty of the hydro-based and energy limited models. Figure from Modirrousta-Galian & Korenaga (in press).

https://doi.org/10.1017/S1743921322004446 Published online by Cambridge University Press

In a forthcoming paper, Modirrousta-Galian & Korenaga (in press) self-consistently incorporate stellar irradiation with atmospheric and geodynamical principles for estimating the mass loss rate of super-Earth and sub-Neptune exoplanets. This combination gives rise to unforeseen emergent properties, such as the three regimes of atmospheric evaporation (see Figure 6). In the first regime, a planet has very high internal temperatures from its high-energy formation processes. These high temperatures give rise to a fully convecting atmosphere that efficiently loses mass without much internal cooling. The second regime applies to planets with lower internal temperatures, so a radiative region forms, but the photosphere still remains outside the Bondi radius. Hence, mass loss continues to depend only on internal temperatures. Planets with the lowest internal temperatures are in the third regime when the photosphere forms below the Bondi radius and mass is lost primarily because of X-ray and ultraviolet irradiation. Modirrousta-Galian & Korenaga (in press) provide the first unifying framework for modeling mass loss through the lifespan of super-Earth and sub-Neptune exoplanets that describes the circumstances at which photoevaporation and core powered mass loss occur. Indeed, the framing of the question should not be whether one mechanism is responsible or the other, but rather when one mechanism is active versus the other.

References

Ahrens, T. J. 1993, Annual Review of Earth and Planetary Sciences, 21, 525
Armitage, P. J. 2014, Lecture Notes on the Formation And Early Evolution of Planetary Systems (CreateSpace Independent Publishing Platform)
Baraffe, I., Alibert, Y., Chabrier, G., & Benz, W. 2006, A&A, 450, 1221
Batalha, N. M., Borucki, W. J., Bryson, S. T., et al. 2011, ApJ, 729, 27
Becker, A., Lorenzen, W., Fortney, J. J., et al. 2014, ApJS, 215, 21
Benatti, S., Damasso, M., Borsa, F., et al. 2021, A&A, 650, A66
Benatti, S., Nardiello, D., Malavolta, L., et al. 2019, A&A, 630, A81
Biersteker, J. B. & Schlichting, H. E. 2019, MNRAS, 485, 4454
Biersteker, J. B. & Schlichting, H. E. 2021, MNRAS, 501, 587
Borucki, W. J., Koch, D. G., Basri, G., et al. 2011, ApJ, 736, 19
Burke, C. J., Bryson, S. T., Mullally, F., et al. 2014, ApJS, 210, 19
Caldiroli, A., Haardt, F., Gallo, E., et al. 2021, A&A, 655, A30
Cameron, A. G. W. 1983, Icarus, 56, 195
Cohen, O., Kashyap, V. L., Drake, J. J., Sokolov, I. V., & Gombosi, T. I. 2011, ApJ, 738, 166
Erkaev, N. V., Kulikov, Y. N., Lammer, H., et al. 2007, A&A, 472, 329
Fulton, B. J., Petigura, E. A., Howard, A. W., et al. 2017, AJ, 154, 109
García Muñoz, A. 2007, Planetary and Space Science, 55, 1426
Genda, H. & Abe, Y. 2005, Nature, 433, 842
Ginzburg, S., Schlichting, H. E., & Sari, R. 2018, MNRAS, 476, 759
Hazra, G., Vidotto, A. A., Carolan, S., Villarreal D'Angelo, C., & Manchester, W. 2022, MNRAS, 509, 5858
Howard, A. W., Marcy, G. W., Johnson, J. A., et al. 2010, Science, 330, 653
Hunten, D. M., Pepin, R. O., & Walker, J. C. G. 1987, Icarus, 69, 532
Ida, S. & Lin, D. N. C. 2004, ApJ, 604, 388
Ida, S. & Lin, D. N. C. 2005, ApJ, 626, 1045
Ikoma, M. & Hori, Y. 2012, ApJ, 753, 66
Ikoma, M., Nakazawa, K., & Emori, H. 2000, ApJ, 537, 1013
Karato, S.-I. 2014, Proceedings of the Japan Academy, Series B, 90, 97
Kubyshkina, D., Fossati, L., Erkaev, N. V., et al. 2018a, ApJ Letters, 866, L18
Kubyshkina, D., Fossati, L., Erkaev, N. V., et al. 2018b, A&A, 619, A151
Lee, E. J., Chiang, E., & Ormel, C. W. 2014, ApJ, 797, 95
Libby-Roberts, J. E., Berta-Thompson, Z. K., Désert, J.-M., et al. 2020, AJ, 159, 57

Lock, S. J., Stewart, S. T., Petaev, M. I., et al. 2018, Journal of Geophysical Research (Planets), 123, 910
Mayor, M. & Queloz, D. 1995, Nature, 378, 355
Micela, G., Cecchi-Pestellini, C., Colombo, S., Locci, D., & Petralia, A. 2022, Astronomische Nachrichten, 343, e10097
Miyazaki, Y. & Korenaga, J. 2019, Journal of Geophysical Research (Solid Earth), 124, 3399
Modirrousta-Galian, D., Locci, D., & Micela, G. 2020, ApJ, 891, 158
Mordasini, C., Alibert, Y., Klahr, H., & Henning, T. 2012, A&A, 547, A111
Nakajima, M. & Stevenson, D. J. 2015, Earth and Planetary Science Letters, 427, 286
Owen, J. E. & Lai, D. 2018, MNRAS, 479, 5012
Owen, J. E. & Wu, Y. 2013, ApJ, 775, 105
Owen, J. E. & Wu, Y. 2017, ApJ, 847, 29
Schlichting, H. E., Sari, R., & Yalinewich, A. 2015, Icarus, 247, 81
Solomatov, V. 2015, in Treatise on Geophysics (Second Edition), second edition edn., ed. G. Schubert (Oxford: Elsevier), 81–104
Tian, F. 2015, Annual Review of Earth and Planetary Sciences, 43, 459
Venturini, J., Guilera, O. M., Haldemann, J., Ronco, M. P., & Mordasini, C. 2020, A&A, 643, L1
Watson, A. J., Donahue, T. M., & Walker, J. C. G. 1981, Icarus, 48, 150
Zeng, L., Jacobsen, S. B., Sasselov, D. D., et al. 2019, PNAS, 116, 9723